boundary into the outgoing state χ_p^+. The initial momentum parallel to boundary of $\hbar(\mathbf{p}+\mathbf{g}_\perp)$ changes to $\hbar\mathbf{p}$ after reflection and the initial normal momentum

$$-\hbar[\tfrac{1}{2}g_z(1+\beta)-\Delta k_z^-]$$

changes to $\hbar[\frac{1}{2}g_z(1-\beta)+\Delta k_z^+]$. We note that the tangential momentum of the electron is not conserved on reflection but can be taken up by the lattice and the amplitude of the incoming and outgoing states are not equal. In fact, the ratio of the amplitudes of the incoming and outgoing states satisfy Eq. (17′), remembering that the velocity in the z direction for this state is given by $\hbar k_z/m$ and using the NFEA that $V_g/Kg^2 \ll 1$. As discussed in Sec. III, this inequality of the amplitudes of the incoming and outgoing states produces a distortion of the distribution of electrons with more electrons moving parallel to the boundary than expected in the interior.

PHYSICAL REVIEW VOLUME 162, NUMBER 1 15 OCTOBER 1967

de Haas–van Alphen Effect and Fermi Surface in Thorium

A. C. THORSEN, A. S. JOSEPH, AND L. E. VALBY
North American Aviation Science Center, Thousand Oaks, California
Received 7 June 1967)

de Haas–van Alphen effect studies have been carried out on the actinide metal thorium. Although sample purities were quite low, two groups of oscillations could be observed throughout the {110} and {100} symmetry planes. These data suggest that the Fermi surface consists of at least a closed segment situated at the point Γ in the center of the Brillouin zone and a set of six closed segments located along the ⟨100⟩ axes at the symmetry point X.

INTRODUCTION

DURING the past decade our understanding of the electronic structure of metals has been greatly enhanced by experiments[1] which investigate the de Haas–van Alphen (dHvA) effect and magnetoresistance behavior. From the results of these experiments and improved band calculations, there has emerged an understanding not only of nontransition metals but also of the more complicated transition metals such as Mo, W, and Re. The ferromagnetic and antiferromagnetic metals have also been studied by such techniques, and much has been learned about the properties of the conduction electrons in these metals. Because of sample purification problems, no such experiments have been reported on the rare-earth metals, although many of their other physical properties have been intensively investigated.[2]

Thorium is perhaps one of the simplest of the actinide rare-earth metals. The electronic configuration of the free atom is $6d^27s^2$ and below $\sim$1400°C the crystalline form has a face-centered-cubic structure. Th, like fcc Pb, has four valence electrons, but from what we already know of the properties of transition metals we expect that the Fermi surface of Th will most likely not resemble that of Pb which is nearly free-electron-like. In this paper, we report on a study of the dHvA effect in Th which constitutes the first detailed study of the Fermi surface of an actinide metal. We find that the Fermi surface consists of at least two types of closed segments, one type lying along the ⟨100⟩ symmetry axes and the other at the center of the Brillouin zone.

EXPERIMENTAL

The data were obtained with conventional pulsed field apparatus which can generate magnetic fields up to 200 kG. Descriptions of the experimental equipment can be found in previous publications.[3] The problem of sample preparation in Th is complicated by the existence of a phase transformation at 1400°C from the high temperature bcc structure to the low-temperature fcc structure. Starting material obtained from Metal Hydrides in the form of crystal bar was arc-melted in an argon atmosphere and rolled out in the form of strips, approximately 0.030 in. thick and 0.35 in. wide. Some of the strips were zone annealed just below the melting point in a Westinghouse induction furnace at a pressure $\approx 10^{-7}$ mm Hg, then strained and reannealed near 1400°C. This procedure yielded strips containing single crystal grains with maximum dimensions up to 0.25 in. Although the resistivity ratios were less than 100, the crystals obtained were suitable for dHvA studies. Other strips were annealed in a high-vacuum furnace by ohmic heating at temperatures just below the phase transformation, and at pressures below

[1] A bibliography of recent experimental and theoretical work in this field may be found in *Proceedings of the Ninth International Conference on Low-Temperature Physics, Columbus, Ohio,* edited by J. G. Daunt *et al.* (Plenum Press, Inc., New York, 1965), pp. 680, 698.

[2] See, for example, *Proceedings of the Fourth Conference on Rare-Earth Research,* edited by L. Eyring (Gordon and Breach Science Publishers, Inc., New York, 1965).

[3] A. C. Thorsen and A. S. Joseph, Phys. Rev. **131**, 2078 (1963), and references therein.

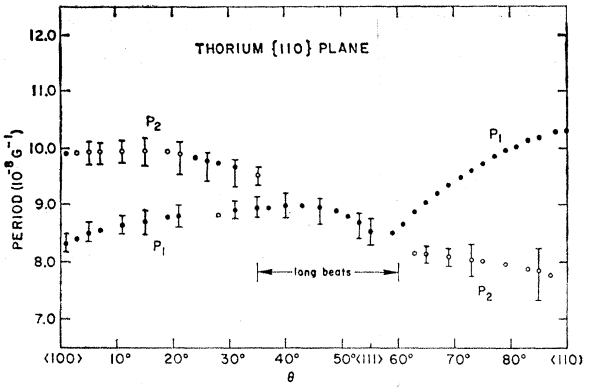

FIG. 1. dHvA periods P_1 and P_2 in thorium in the {110} plane. Solid circles denote periods of the dominant oscillations and open circles denote periods derived from beats. The data represent the averaged results from three samples. The error bars indicate the range of scatter between different samples or from a particular sample. These periods are associated with a set of six ellipsoids located at the symmetry points X.

10^{-8} mm Hg. The one sample obtained in this way gave comparable dHvA amplitudes. Single-crystal samples were spark cut from the annealed strips in the form of rectangular bars having typical dimensions $\sim 0.02 \times 0.03 \times 0.1$ in.[3]. Three samples were used in this experiment; the axis of one sample was along [111], the axis of the second was along [100], and the third sample had its axis located 16° from the [100] direction in the (110) plane. Data were taken in both the (100) and (110) planes.

RESULTS AND DISCUSSION

The angular variations of the dHvA periods are plotted in Figs. 1–4. In all cases the angle θ is measured from the [100] axis in the (110) plane and the angle φ is measured from the [100] axis in the (100) plane. The data can be separated into two groups according to the magnitudes of the periods. The first group comprising

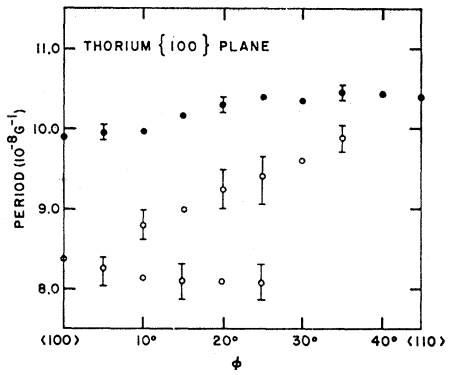

FIG. 2. dHvA periods in thorium in the (100) plane. Solid circles denote periods of the dominant oscillations, and open circles denote periods derived from beats. The data represent the averaged results from one sample with the scatter indicated by the error bars. These periods are associated with a set of six ellipsoids located at the symmetry points X.

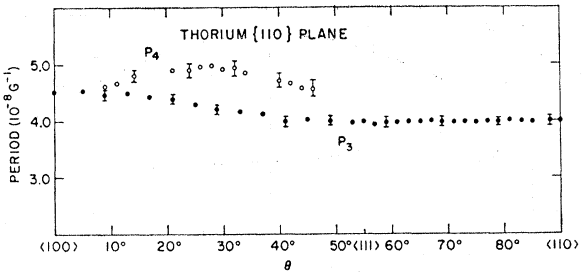

FIG. 3. dHvA periods P_3 and P_4 in thorium in the (110) plane. Solid circles denote periods of the dominant oscillations, and open circles denote periods derived from beats. The data represent the averaged results from two samples. These periods are associated with a nearly spherical-Fermi surface segment located at the symmetry point Γ.

the larger period data taken in the (110) and (100) planes is represented in Figs. 1 and 2, respectively. In the (110) plane, the data appear to have two branches, labeled P_1 and P_2. Along the [100] axis the two period values are 9.9 and 8.3×10^{-8} G^{-1}. These two periods approach each other as θ increases and appear to merge near [111]. For $\theta > 55°$, P_1 increases rapidly to a value of 10.3×10^{-8} G^{-1} along [110], and the amplitudes of the oscillations increase. The amplitude of the lower branch P_2 diminishes and finally vanishes about 5° from [110]. The amplitudes of the oscillations are very small over most of the plane which accounts for the large scatter in the data. In the region $27° > \theta > 22°$ the branch P_1 actually vanishes.

In the (100) plane the two periods observed along [100] apparently split into three branches as the field is rotated toward [110]. The oscillations related to the upper branch are dominant throughout the plane while the oscillations corresponding to the lower branch are quite weak and disappear near [110]. The middle branch can be observed from $\varphi \approx 10°$ to $\varphi \approx 35°$. This branch appears to join the upper branch at the [110] axis. The angular variations of P_1 and P_2 suggest that these periods can be associated with ellipsoidal energy

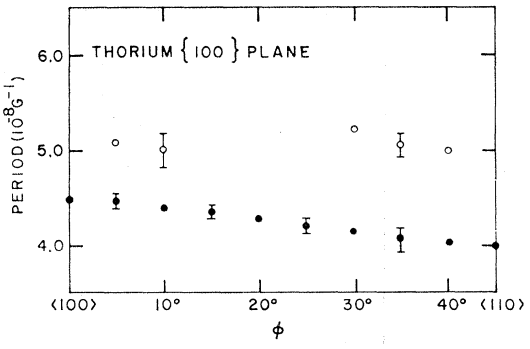

FIG. 4. dHvA period data in thorium in the (100) plane obtained from one sample. Solid circles denote periods of the dominant oscillations and open circles denote periods derived from beats. These periods are associated with a nearly spherical Fermi surface segment located at the symmetry point Γ.

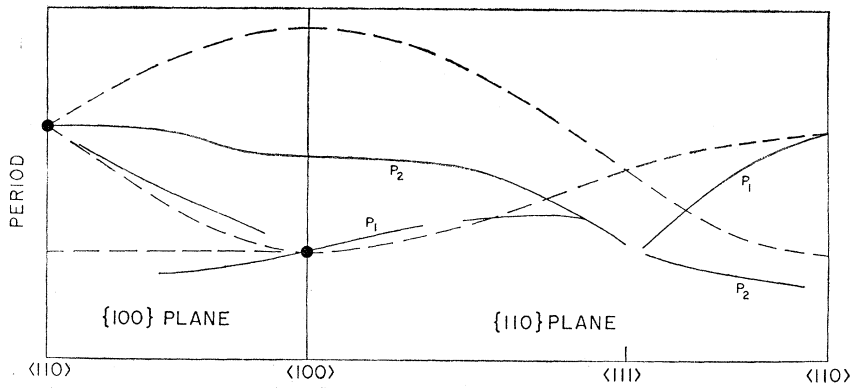

FIG. 5. Comparison of the experimental data (solid curves) with those expected from a set of six ellipsoids (dashed curves) located along the ⟨100⟩ axes. The dashed curves have been normalized to P_1 along the ⟨100⟩ and ⟨110⟩ axes.

surfaces. In Fig. 5, we plot the periods versus angle for a set of six ellipsoids situated at the symmetry points X of the Brillouin zone and oriented so that their major axes are along the ⟨100⟩ directions. The values of the periods associated with these ellipsoids are normalized to agree with P_1 along the ⟨100⟩ and ⟨110⟩ directions. It can be seen that the major differences are a depression of the upper branch of the experimental data around ⟨100⟩, and of the branch P_1 near ⟨111⟩. Another significant difference is the disappearance of the lower branch near the ⟨110⟩ axes. We suggest that the data can be accounted for by distorted ellipsoids, as shown in Fig. 6. We have sketched an ellipsoid with major axis along ΓX and have located the center of the ellipsoid at the point X. The distortions necessary to explain the data consist of four bulges around the equator of the ellipsoid pointing along the lines XW. We have tentatively located the ellipsoids at the points X in the Brillouin zone, although on the basis of the data themselves the ellipsoids could be located at different positions along the ΓX line between Γ and X. If we assume an ellipsoidal shape, we obtain a value of 0.026 Å^{-3} for the volume of each ellipsoid, and an effective volume inside the zone of 0.078 Å^{-3} if the segments are centered at the point X.

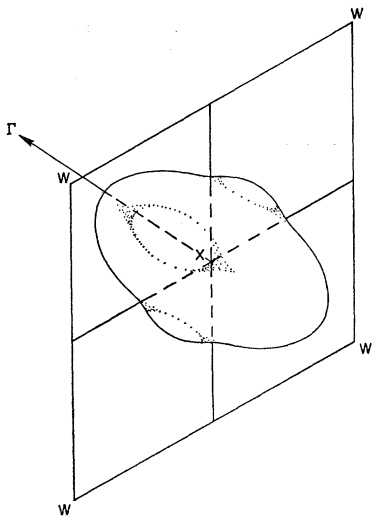

FIG. 6. Schematic model of a distorted ellipsoidal Fermi surface segment located at the symmetry point X which can account for the periods P_1 and P_2.

The disappearance of P_2 near the [110] axis and P_1 near $\theta \approx 25°$ in the (110) plane cannot be accounted for by a topological feature of our model; however, it is well known that spin-splitting effects may cause the amplitude of the dHvA oscillations to vanish for some combinations of effective mass and electron g-factor values.[4] We have studied the amplitudes of the oscillations associated with the branch P_1 along the [110] axis as a function of temperature and have deduced a value of $m^* = 0.33\, m_0$. From previous experience we have found that values of effective mass obtained from our pulsed field measurements have been from 20–30% low, so we can estimate that the true mass is $\sim 0.4\, m_0$. Consequently, if the g value is nearly 2, a mass of this order would result in small amplitudes, and could account for the weak oscillations observed for most field directions. We therefore tentatively associate the disappearance of the oscillations along the above mentioned field directions with spin-splitting effects.

The second group of data observed in Th is plotted in Figs. 3 and 4 in the (110) and (100) planes, respectively. Throughout these two symmetry planes there is only one dominant branch P_3 in the smaller period data. The period values vary only slightly in the two planes, ranging from 4.5×10^{-8} G^{-1} along the [100] axis, to 4.0×10^{-8} G^{-1} along [110]. An additional branch P_4 was observed in the (110) plane (Fig. 3) and appears to join P_3 at the [100] axis. The period P_4 cannot be followed all the way to [110] but appears to approach P_3 near the [111] direction.

In the (100) plane, only one branch of the data can be followed. However, there is evidence of another period which can be associated with the second harmonics of the larger periods P_1 and P_2 discussed above. The amplitudes of the P_3 oscillations are very weak throughout most of the plane but increase by a factor of 4 near the [100] axis. Along this axis the temperature

dependence of the amplitude of the oscillations yields a value (corrected as before) of effective mass $m^* \sim 0.6 m_0$.

The data shown in Figs. 3 and 4 are suggestive of a nearly spherical closed piece of Fermi surface. The fact that only one branch is observed through most of the two planes indicates in addition that there is only one segment of the surface in the Brillouin zone, which therefore must be centered at the point Γ. With this assignment, the two branches of data observed in the (110) plane near the [100] axis must necessarily arise from two extremal orbits on the same surface. The merging of these two branches may account for the large amplitudes of P_3 observed near the [100] direction, a possibility discussed by Pippard.[5] We find that a sphere which has large bulges in the ⟨111⟩ directions, slightly smaller bulges along the ⟨110⟩ directions, and indentations along the ⟨100⟩ directions can qualitatively account for the observed behavior of the dominant period. Such a model furthermore could lead to multiple extremal orbits near the ⟨100⟩ axes, and hence account for P_4.

Approximating this surface by a spherical topology corresponding to an average period of 4.2×10^{-8} G^{-1}, we estimate the relevant volume to be 0.082 Å^{-3}. This is 1.1% of the zone volume and is approximately equal to the effective volume of the ellipsoids inside the zone as mentioned above.

The Fermi surfaces deduced from existing band calculations[6,7] are not in accord with the model proposed above. The earlier work by Lehman, however, does predict small hole pockets located along the ⟨100⟩ axes between Γ and X, and a smaller electron pocket centered at Γ. The volumes associated with these hole and electron pockets are $\sim 2.6\%$ and 0.2% of the zone volume, respectively. These calculations, on the other hand, also predict pockets along the ⟨110⟩ and ⟨111⟩ axes, although no evidence for these was found in this investigation. The interpolation model used by Lehman neglects the influence of the $7s$ and $5f$ orbitals and it is possible that any agreement between the experimentally deduced Fermi surface and the above mentioned theoretical predictions is fortuitous. According to Loucks,[8] the $5f$ orbitals may play a far more important role in thorium than previous relativistic augmented-plane-wave (RAPW) calculations[7] indicated. In fact, he feels that it will be necessary to make the entire calculation self-consistent for the solid in order to obtain accurate Fermi surfaces.

In conclusion, we have studied two sets of de Haas–van Alphen periods in the {100} and {110} symmetry planes. The larger period data can be attributed to a set of six slightly distorted ellipsoids located at the point X in the Brillouin zone with their major axes along ΓX. The short period data are interpreted as being a consequence of a nearly spherical segment of Fermi surface located at the center of the zone. From the volumes of these segments, we estimate that only 0.04 carriers per atom are responsible for the oscillations associated with P_1 through P_4. This is a small number indeed, but in view of the fact that the amplitudes of the oscillations were quite small even at 180 kG, it is quite possible that other large segments of the Fermi surface were not detectable because of their low $\omega_c \tau$. Thus, a more complete picture of the Fermi surface will require preparation of thorium samples of much higher purity.

Note added in proof. The data in the (110) plane, Fig. 1, bear some resemblance to those obtained on Pb[9] and Al.[10,11] In Fig. 1, P_1 for $55° < \theta < 90°$ can be fitted to a cylindrical Fermi surface. For these reasons it has been suggested[12] that the periods P_1 and P_2 are possibly associated with cylindrical surfaces at the symmetry points K and pointing in the ⟨110⟩ directions. However, the fact that the general behavior of the data in the (100) plane, Fig. 2, is shifted 45° from those in Pb and Al is strong argument against such a possibility.

ACKNOWLEDGMENTS

The authors express their gratitude to H. Nadler and P. Q. Sauers for spending a great deal of time and effort to develop the techniques for the preparation of the samples used in this investigation. They thank D. Swarthout for orienting the crystals, T. G. Berlincourt for a critical reading of the manuscript, and G. W. Lehman for helpful discussions.

[4] A. S. Joseph and A. C. Thorsen, Phys. Rev. **134**, A979 (1964); A. S. Joseph, A. C. Thorsen, E. Gertner, and L. E. Valby, *ibid.* **148**, 569 (1966).

[5] A. B. Pippard, *The Dynamics of Conduction Electrons* (Gordon and Breach Science Publishers, Inc., New York, 1965), p. 103 ff.

[6] Guy W. Lehman, Phys. Rev. **116**, 846 (1959); *Progress in Nuclear Energy*, edited by H. M. Finniston and J. P. Howe (Pergamon Press, Inc., New York, 1959), Series V, Vol. 2, p. 570.

[7] S. C. Keeton and T. L. Loucks, Phys. Rev. **146**, 429 (1966).

[8] T. L. Loucks (private communication).

[9] A. V. Gold, Phil. Trans. Roy. Soc. London **251**, 85 (1958). Also, J. R. Anderson and A. V. Gold, Phys. Rev. **139**, A1459 (1965).

[10] E. M. Gunnersen, Phil. Trans. Roy. Soc. London **A249**, 299 (1957).

[11] W. A. Harrison, Phys. Rev. **116**, 555 (1959).

[12] W. A. Harrison (private communication).